Int J Adv Manuf Technol (2017) 89:3257–3269
DOI 10.1007/s00170-016-9297-6

ORIGINAL ARTICLE

Manufacturing metallic bipolar plate fuel cells through rubber pad forming process

Majid Elyasi[1] · **Farzad Ahmadi Khatir**[1] · **Morteza Hosseinzadeh**[2]

Received: 29 August 2015 / Accepted: 4 August 2016 / Published online: 17 August 2016

Abstract Bipolar plates are considered one of the most important parts of fuel cells, made of different materials. Graphite bipolar cells are generally expensive, hence high machining cost. Metals are known to be suitable replacements due to their lower weight and cost. Bipolar plates can be designed and produced using either a concave or convex pattern. This study made an effort to fabricate metallic bipolar plates through two-die rubber pad forming method with both convex and concave patterns. Stainless steel sheets of 316 with the thickness of 0.1 mm were used for the fabrication. Polyurethane with the hardness of shore A 85 and the thickness of 25 mm was selected. The effect of forming forces on micro-channel filling depth, thickness distribution of channels in each of the patterns, and their appropriate states (maximum filling depth and minimum thickness reduction) were also studied. The results indicated that in similar geometry and process, the convex die would create a deeper channel compared with the concave one. Increases in forming forces would cause the filling depth of micro-channels to rise, but the thickness of critical regions to decrease due to an increase in the aspect ratio (the ratio of channel depth to channel width). Finally, the best possible version of bipolar plates in both convex and concave models was formed.

Keywords Rubber pad forming · Convex and concave die patterns · Metal bipolar plates · Fuel cells

✉ Majid Elyasi
elyasi@nit.ac.ir; elyasima@yahoo.com

[1] Department of Mechanical Engineering, Babol Noshirvani University of Technology, P.O. 484, Babol, Mazandaran, Iran

[2] Department of Mechanical Engineering, Ayatollah Amoli Branch, Islamic Azad University, Babol, Mazandaran, Iran

1 Introduction

Nowadays, fuel cells are being shown to be a suitable replacement for internal combustion engines. Since fuel cells produce chemical electricity, their efficiency in producing energy would be much better than combustion. Other advantages of fuel cell technology are its compatibility with the environment as it causes no sound pollution and is capable of producing heat and electricity simultaneously [1].

Bipolar plates are one of the most important parts of fuel cells responsible for gathering the external flow of cathode and anode. They are also considered tools for distributing fuel flow in anode and air or oxygen in cathode; cooling fluid also flows in them. However, the distribution of reactive gases could be implemented with grooves created on their surface [1].

In general, bipolar plates make around 75 % of a cell weight and 11 to 45 % of its price. To reduce the total weight and price, and increase the efficiency and life time of a fuel cell, choosing an appropriate production method would undoubtedly play a crucial role, as well as the quality of materials [2, 3].

Different methods have been proposed to create tracks on bipolar plates. One of the most common ones is graphite plate machining. Graphite is known for its electric conductivity, ease of machining, and lower density compared with metals. However, this method was shown to entail the following drawbacks [4]:

1. Cutting graphite requires spending much time on costly systems.
2. Graphite is fragile, which means there would be the possibility of breaking, being undermined during cutting process or producing fuel cells in series.
3. Although graphite plates have the ability to separate different reactive gases, they must have a thickness of a few

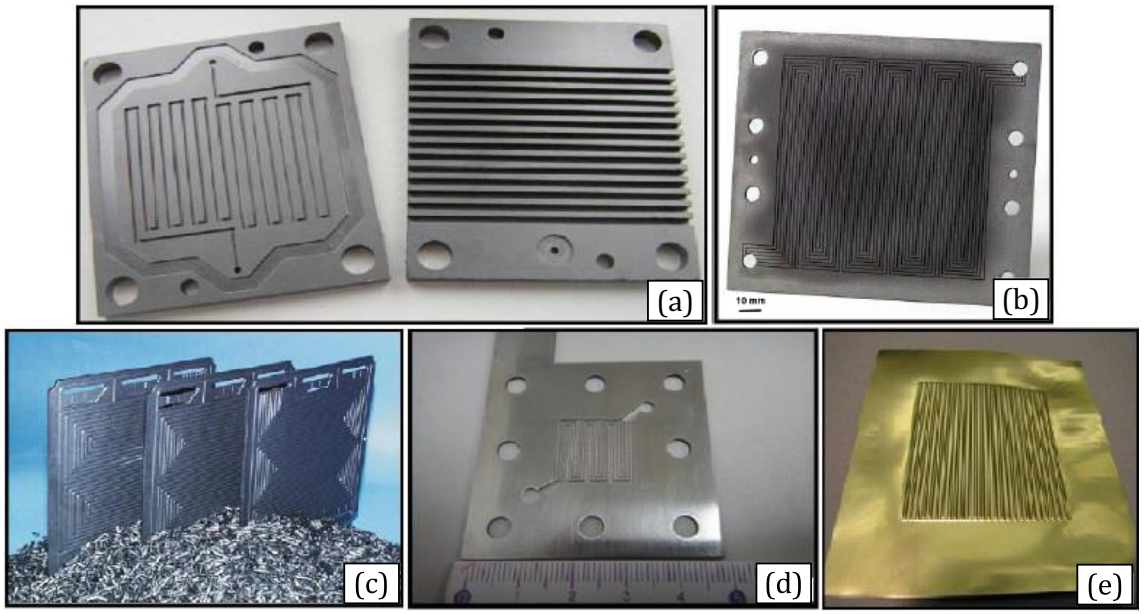

Fig. 1 Different types of bipolar plates produced by different methods: **a** machined graphite, **b** molded carbon/carbon material, **c** molded polymer/carbon composite, **d** micro-EDM stainless steel, and **e** forming stainless steel [6]

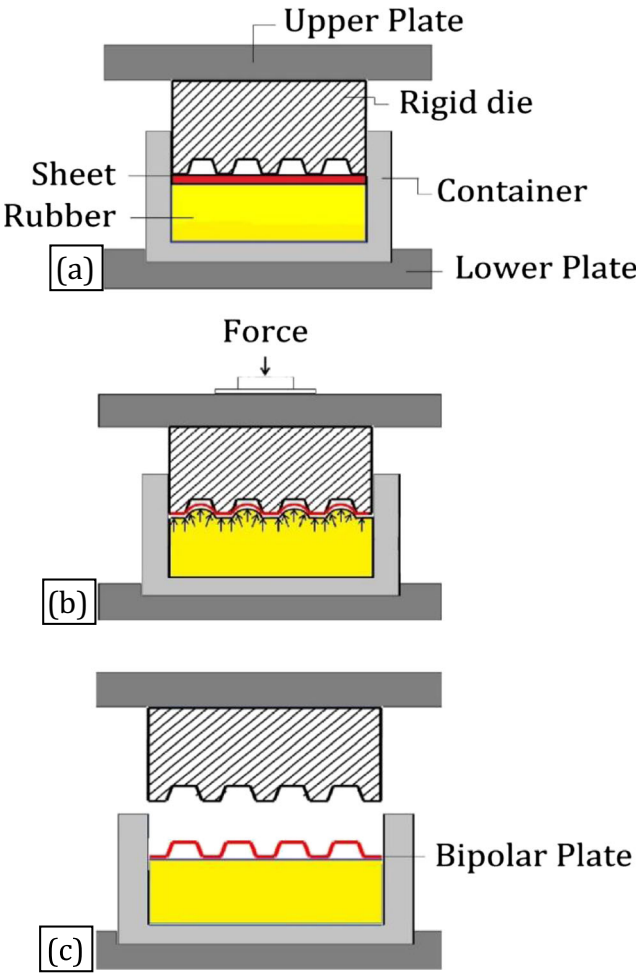

Fig. 2 Schematic diagram of rubber pad forming process, **a** stage one, **b** stage two, and **c** stage three

millimeters. Thus, despite the fact that the density of their material is low, the total weight of them is not necessarily low.

In addition to graphite, some metals are used to produce bipolar plates. Using metals could bring the following advantages [4]:

1. Metals are formed more easily.
2. Metals do not contain surface porosity, as a result, thin pieces of metal can keep reactors apart from each other.

The biggest problem with metals is their high density and weakness against corrosion. To form bipolar plates, there are different forming methods, such as electromagnet forming, laser forming, hydroforming, gas forming, stamping, and rubber pad forming [5]. Figure 1 shows different types of bipolar plates produced by different methods.

One of the most common methods of forming metallic plates is rubber pad forming process. In this method, rubber

Table 1 Sheet chemical compounds according to the weight of elements

Cr	Cu	V	Nb	Sn	S
16.15	0.36	0.09	0.002	0.023	0.005
Mn	Si	Al	W	Fe	C
1.44	0.66	0.01	0.071	Base	0.047
P	Co	Ti	Ni	Mo	Pb
0.048	0.28	0.04	12.19	2.11	0.01

Table 2 Mechanical properties of stainless steel 316 sheet

Mechanical properties	Value
Young's modulus (E (GPa))	200
Poisson's ratio (ν)	0.3
Yield stress (σ_y (MPa))	296
K (MPa)	1512
n	0.53
ε_0	0.04

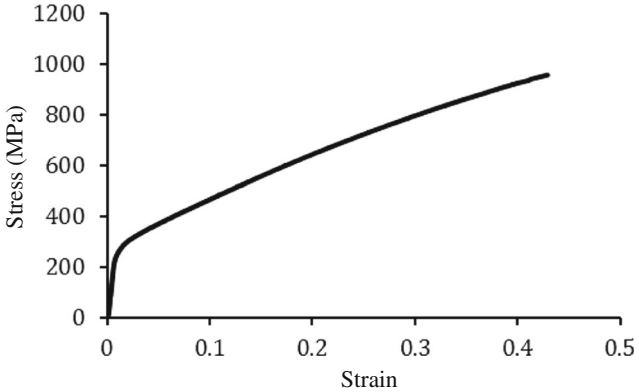

Fig. 4 True stress-strain curve of stainless steel 316

is placed inside a rigid shell which is fastened from sides. Only the upper surface of the rubber touches the plate and die to fill channel cavities. That is why the launching time for this process is shorter and also the equipment is cheaper than the other processes, such as stamping and hydroforming. This would make it a suitable alternative in mass production [7].

Forming process with rubber pads includes three stages. In stage one, the sheet is placed between two-die jaws; the rubber inside the container and between the lower shell, playing the role of a matrix; and convex or concave dies in the upper jaw, playing the role of a plunger. In stage two, the force of a hydraulic stamp is exerted to form the sheet. In this stage, the flexibility of rubber causes the sheet to fill channel cavities. In stage three, the formed sheets are extracted from the die (Fig. 2).

Although using rubber as a tool in forming plates is not very new, there is not enough literature available in this respect. Liu et al. [8] studied the effect of forming patterns on producing bipolar metallic plates (SS304) using rubber pad forming process, creating both convex and concave dies for a single channel of bipolar plates. The influence of these two patterns on filling force and thickness distribution of channels were also researched. The study analyzed the ratio of channel width (w) to channel rib (s) through two-dimensional simulations. The results showed that if the ratio was greater than 1, the concave method would be more efficient, otherwise the convex pattern would be better.

Jeong et al. [9] examined the effect of channel wall angles on filling depth in metal bipolar plates (SS304) at 10°, 20°, and 30°. They also researched processing parameters, such as ram speed and punch pressure. The results indicated that increases in the speed of form changing, punch pressure, and also wall angle would cause filling depths to rise in channels. The dependence of wall angle to punch pressure was also much more than its speed. The most appropriate wall angle obtained was 20°.

Youl son et al. [10] formed aluminum plates (Al 1050) through rubber pad forming process. To conduct the study, some parameters, such as speed, punch pressure in flow channel depths, a die with a convex pattern, and rubbers with different rigidity were utilized. The results illustrated that

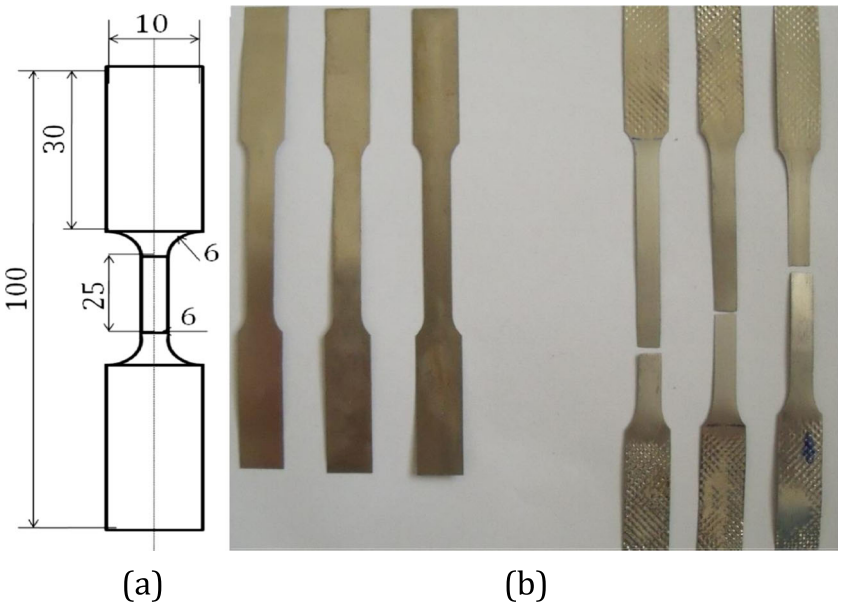

Fig. 3 Tensile test of sheet steel plate stainless steel 316, **a** size of the sample and **b** achieved sample

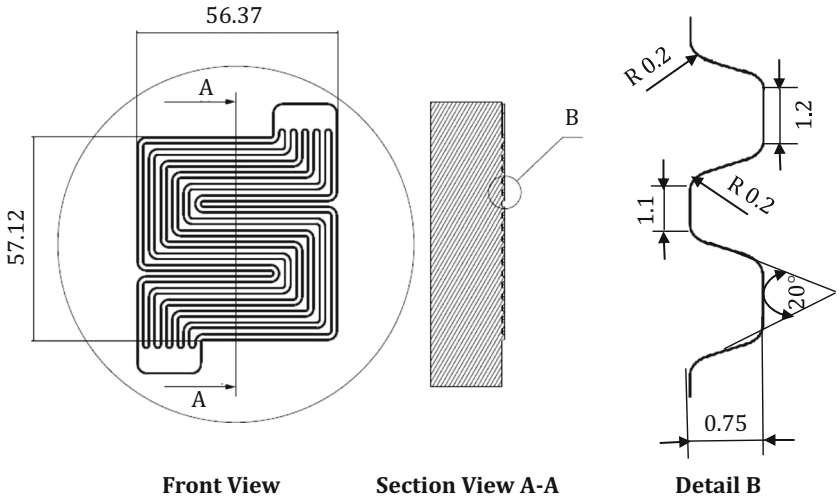

Fig. 5 First groove design and its dimensions and sizes (mm)

increasing speed and pressure would lead to more filling depth in flow channels. The maximum decrease in sheet thickness would increase with rises in punch pressure and speed.

Only reference [8] carried out research into producing a channel using both concave and convex dies. However, the study concentrated on single channels only. It is notable that when the number of bipolar plate channels increases, forming a bipolar plate can be more difficult than a single channel. Hence, single channel results could not be extended to form a real bipolar plate.

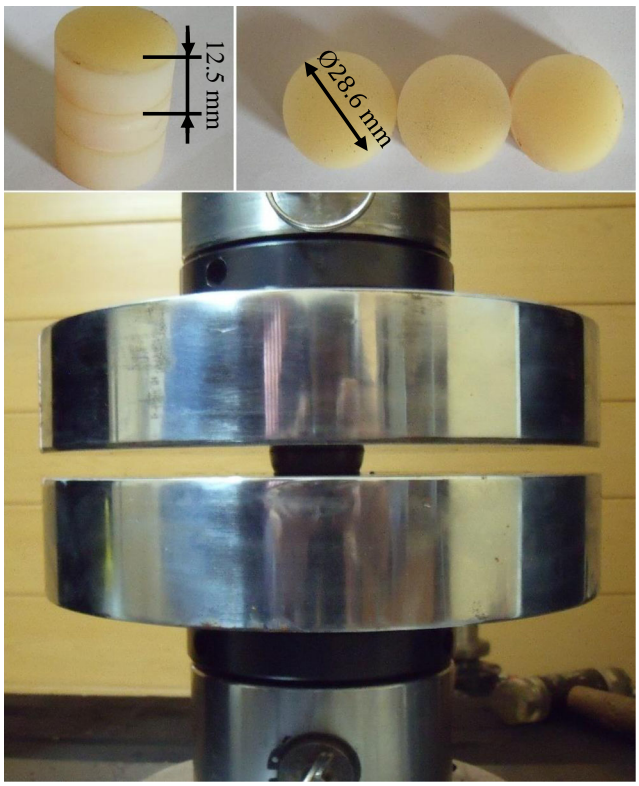

Fig. 6 Samples of rubber pressure test and the applied device

The aim of this research was to produce an industrial scale and industrial form of metallic bipolar plates with serpent grooves using rubber pad forming process. It focused on the effect of die patterns on the final shape of workpieces. In other words, the effect of both convex and concave patterns on the distribution of thickness and uniformity of ribs was studied.

Generally, in these dies as the ratio increases, the formation of bipolar plates can be more complex. Complexity index was defined here as the ratio of depth to width of channel. The selected ratio was 0.7, which was larger than the ratio in previous research.

The complexity index of forming at this ratio clearly showed that the convex pattern would be better than the concave one since a deeper pattern was created in the convex pattern, and distribution of bipolar plates was also acceptable.

2 Experimental setup and methodology

Stainless steel 316 sheet with the thickness of 0.1 mm was used due to being more resistant to corrosion compared with other austenitic plates, an important factor in metal plate discussion. Table 1 shows chemical compounds of the utilized sheets according to the weight of their elements.

Table 3 Rubber characteristic test

Parameter	Value
Rubber kind	Polyurethane
Rubber hardness	Shore A 85
Velocity test	1 mm/s
Machine type	SANTAM250
Sample diameter	12.5 mm
Sample height	28.6 mm
Number of samples	3

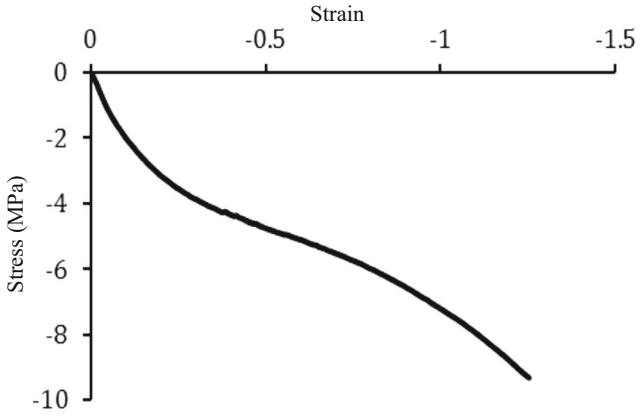

Fig. 7 Compression curve according to polyurethane rubber

The behavior of plastic material is defined as $\sigma = K(\varepsilon_0 + \varepsilon)^n$. In order to determine the mechanical properties of metal plates, three samples were developed to uniaxial tension test according to ASTM E8M standard (Table 2). Figure 3 shows tension samples before and after tension. Figure 4 illustrates the true stress-strain curve of the sheet in tested samples. The frame of serpent channel and its dimensions are shown in Fig. 5.

According to previous studies, the best compound of wall angle and corner radius was found to be 10° and 0.2 mm, respectively, which were selected in this research as well. However, channel depth was selected in a way to research the initial sheet thickness rubber pad forming process in the most complicated state compared with previous studies.

Using this frame, two similar dies (convex and concave) were made, i.e., the same wall angle and corner radius. A polyurethane (PU) with the hardness of shore A 85 and thickness of 25 mm was used to form metal plates.

To determine the mechanical properties of polyurethane, a sample compression test according to ASTM D575 was provided. In Fig. 6, PU samples and pressure jaws for pressing the PU are shown. Rubber test parameters are shown in Table 3.

As Fig. 6 shows, the standard samples were placed between the two jaws of pressure testing machine, which was attached to a computer system. It showed the momentary data on force to movement. To confirm the results, three samples were prepared. It was observed that stress-strain curves behaved almost similarly in all samples. The true stress-strain curve of PU, obtained from compression test, is illustrated in Fig. 7.

Both convex and concave dies were made from SPK steel and the grooves were machined with a CNC machine accurately. As mentioned, to produce a metallic bipolar plate, either a convex die, having the role of a punch, or a concave one, having the role of a matrix, can be used. Since in rubber pad forming process rubber replaces one of die sides, either convex or concave die could be selected for the other side. This would be effective in producing the final plate.

To investigate the effect of convex and concave forming patterns, only ref. [8] analyzed sheet formability in terms of aspect ratio (w/s) in the channel of bipolar plates, using simulation. However, the study did not consider the formability of anode-cathode surfaces and current paths. Much research has been conducted into the corrosion of metallic bipolar plates. The results showed that in the formed metallic bipolar plates, anode-cathode surfaces (surfaces in contact with MEA) would be highly exposed to corrosion. That is why these regions require high quality [11].

On the other hand, the roughness of deformed areas (peak) would increase faster as forming force rose compared with surfaces in contact with the die (valley) [12]. In this study, in the convex die, current paths were fixed when anode-cathode surfaces were forming. Conversely, in the concave die, anode-cathode surfaces were fixed when current paths were forming (Fig. 8). Therefore, it could be necessary to evaluate filling and thickness distribution in each of these two dies in order to produce the most efficient bipolar plate. In Fig. 9, the two convex and concave dies are shown, whose sizes and dimensions are given in Table 4. In Fig. 10, the constituent parts of the dies are illustrated in a single state.

Figure 11 shows a complete collection of die component assembly in addition to the schematic of its components. Figure 12 illustrates a special hydraulic press machine with the capacity of 100 tons, made by Santam Company. It was

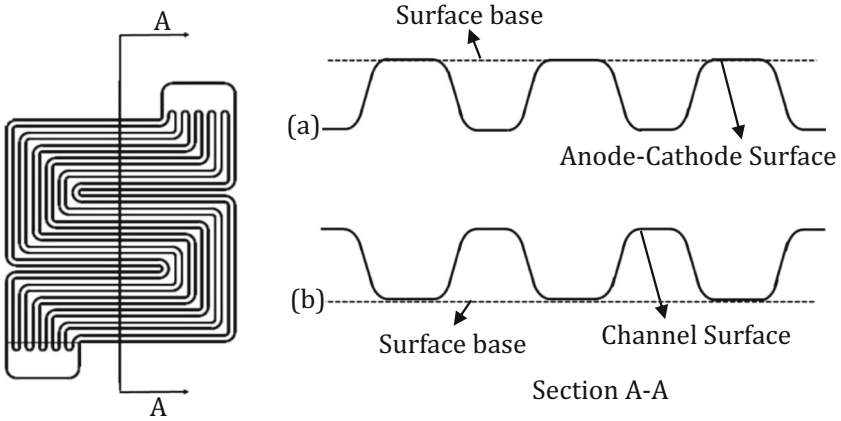

Fig. 8 Sheet formation in both **a** convex and **b** concave dies

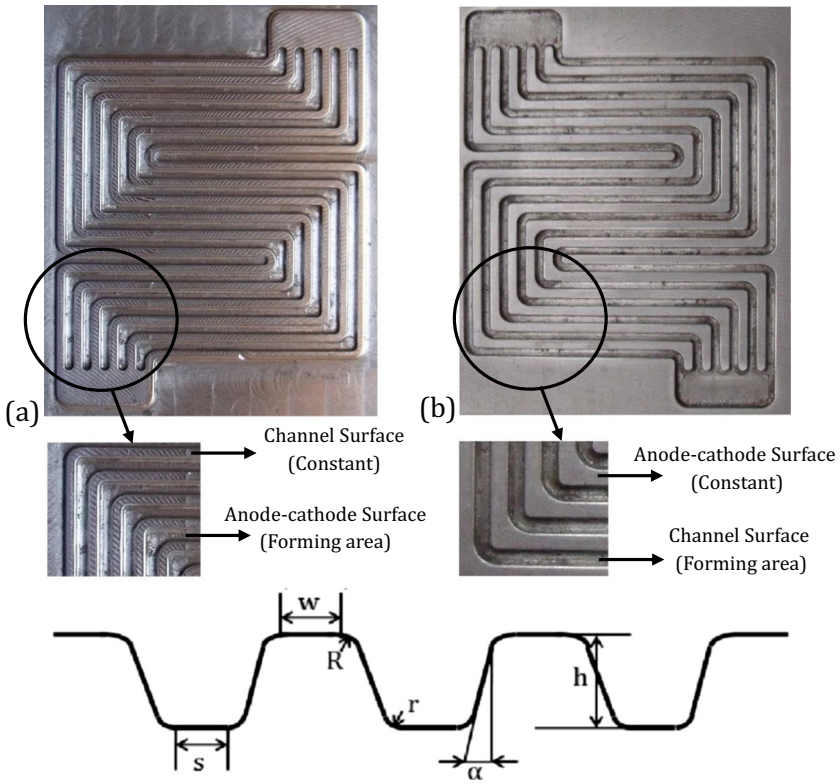

Fig. 9 Geometry of **a** convex and **b** concave dies

used in this study to impose force to the die. To record the output, fully automated computer facilities were embedded into the system. They could print the output in curves or provide a text file with TXT extension. All machine movements could be controlled by the computer connected to it to help adjust progress rate and observe clamping force more exactly, on the path any moment.

To perform the required tests, sheets of various dimensions were cut and adjusted into the die. Different forces (35, 45, 55, and 60 tons) were used to from plates. All tests were done at the same conditions in both convex and concave dies for an accurate comparison. The process parameters for forming plates are illustrated in Table 5.

The formed plates were cut using a wire cut machine to study the distribution of their thickness and filling profile. After that, mounting operation was performed on segmented samples (Fig. 13). The surface was polished to see the profile of the samples accurately under microscope. Firstly, the observation was done under ×2 magnifying power with VMM-VMS measuring device. Subsequently, for higher accuracy, optical microscope of ×4 magnifying was used. Measuring software connected to a computer system and attached to a microscope was used to determine channel filling profiles as well as its thickness distribution.

Table 4 Dimensions and sizes of two produced dies (mm)

Geometric parameters	Concave die	Convex die
Channel width (w)	1.1	1.1
Channel rib (s)	1.2	1.2
Channel depth (h)	0.75	0.75
Top radius (R)	0.2	0.2
Botom radius (r)	0.2	0.2
Channel wall angle (α)	10°	10°

3 Thickness distribution criteria and channel filling data

Maximum thinning was used for the analysis of tearing based on ref. [13], defined by Eq. (1):

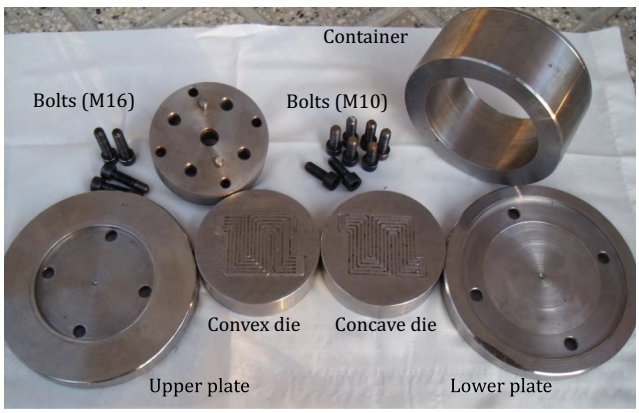

Fig. 10 Die parts in single states

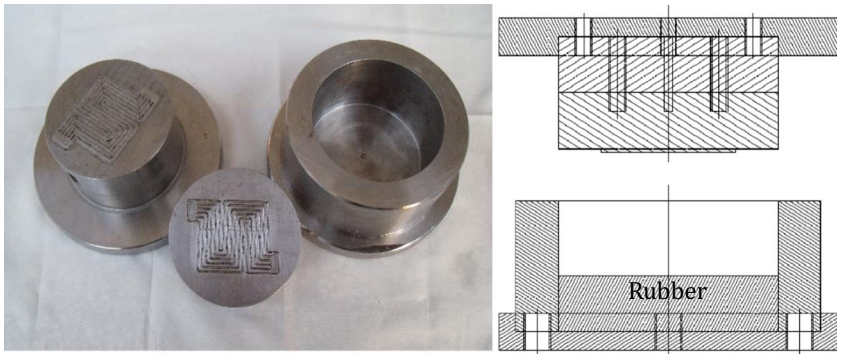

Fig. 11 Die parts in assembly states and a schematic assembly view

$$\text{Thinning percentage} = ((t_0 - t_f)/t_0) \times 100 \quad (1)$$

where t_0 is sheet initial thickness, and final thickness was obtained by Eq. (2):

$$t_f = t_0 \exp(\varepsilon_t) \quad (2)$$

Main engineering strain (e_r) was estimated by Eq. (3) in which n is hardening strain and t_0 is primary thickness [11]. True strain and thickness strain were defined by Eqs. (4) and (5):

$$e_r = [(23.3 + (360/25.4) \times t_0)(n/0.21)] \quad (3)$$

$$\varepsilon_r = \ln(1 + e_r/100) \quad (4)$$

$$\varepsilon_t = -\varepsilon_r \quad (5)$$

Using Eqs. (4) and (5), computing (ε_t), and replacing in Eq. (2), the real value of (t_f) could be reached, and then, maximum thinning computed by Eq. (1).

According to Eq. (1), the maximum thinning of stainless steel 316 sheet was calculated, 38 %. Compared with the experimental results (34 %), there was 4 % difference which could be neglected.

Equation (6) was used to determine the percentage of filling, based on the ratio of filled area of formed channel to the total area of die channel (Fig. 14).

$$\text{Filling percentage} = (\text{filled area of formed channel}/\text{total area of die channel}) \times 100 \quad (6)$$

4 Analyzing results

The effect of force on filling depths and thickness distribution of bipolar plate channels were studied in both convex and concave patterns. The best possible conditions (maximum filling depth and minimum thickness reduction) were obtained in both of them. Forces from 35 to 60 tons were applied to form a bipolar plate at the speed of 5 mm/s. Polyurethane was also used with the hardness of share A 85 and thickness of 25 mm to form the plate.

Fig. 12 Applied stamping device as acting force in the die

5 Filling percentage

The object of this research was to produce a bipolar plate with maximum filling depth and to survey die patterns on the formed plates. Maximum filling percentage and thickness distribution of bipolar plate channels were studied both longitudinally and diagonally.

Figure 15 shows filling depth of bipolar plate channels along a longitude path in both convex and concave dies at

Table 5 Processing parameters for forming plates

Process parameters	Concave die	Convex die
Forming temperature (°C)	25	25
Forming forces (ton)	35, 45, 55, and 60	35, 45, 55, and 60
Forming velocity (mm/s)	5	5

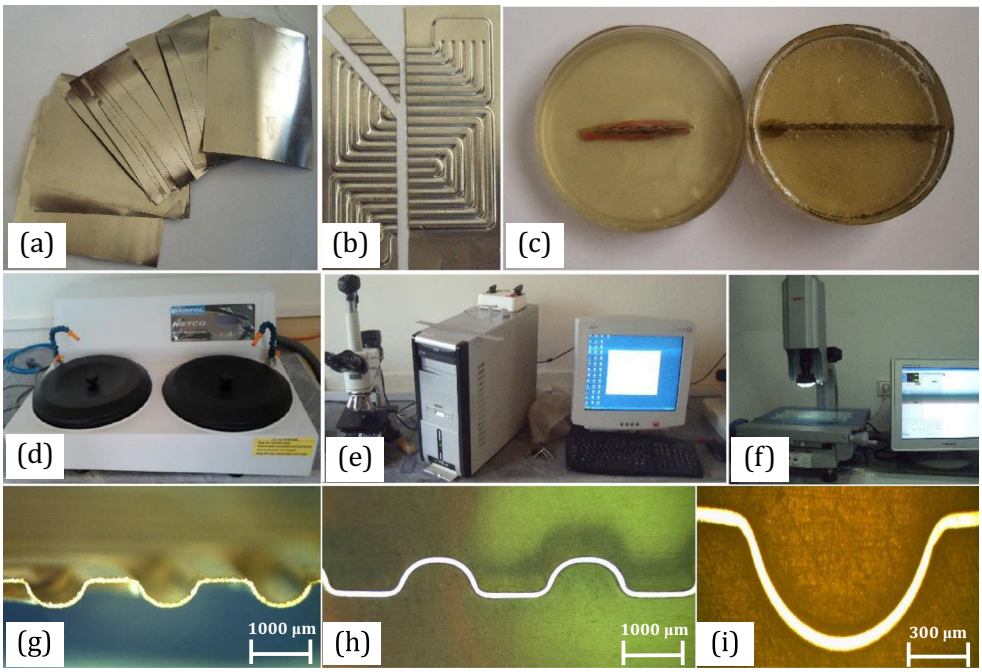

Fig. 13 Preparation stages of formed samples to survey thickness distribution and filling profile of samples, **a** raw material, **b** sheet cutting in longitudinal and cross-sectional directions, **c** mounting longitudinal and cross-sectional samples to see the profile under microscope, **d** special rotational device for polishing mounted samples, **e** microscope to see mounted profile with ×4 magnifying and measuring samples, **f** measuring VMM-VMS device to see mounted profile with ×2 magnifying, **g** VMM-VMS image without polish, **h** VMM-VMS image with polish, **i** microscopy image of channel die

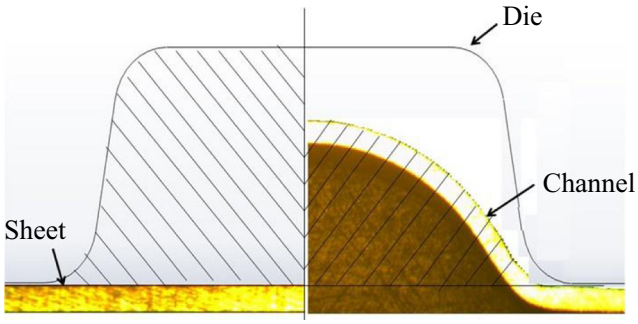

Fig. 14 A view of formed sheet area and die channel area

35 to 60 tons. As can be seen, increasing the force can cause the filling depth in channels to rise in both convex and concave dies. However, the convex die produced more filling depth compared to the concave one. This could be explained by the convex die having smaller touching surface with the sheet due to lower channel width and higher rib width (Table 4). It created more space for the rubber to conduct the

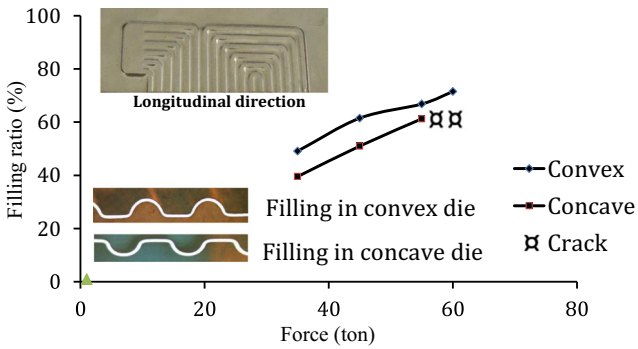

Fig. 15 Depth of channel filling in both convex and concave dies, longitudinally

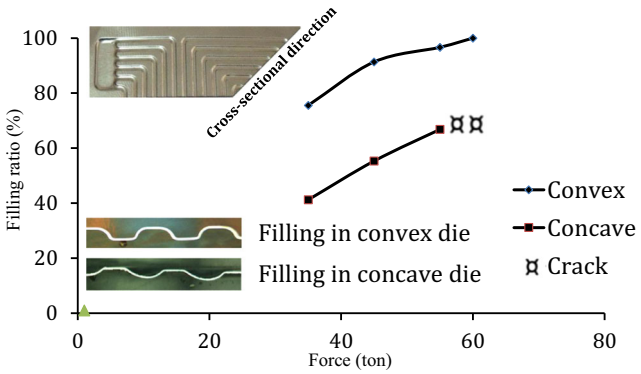

Fig. 16 Depth of channel filling in both convex and concave dies at cross-sectional direction

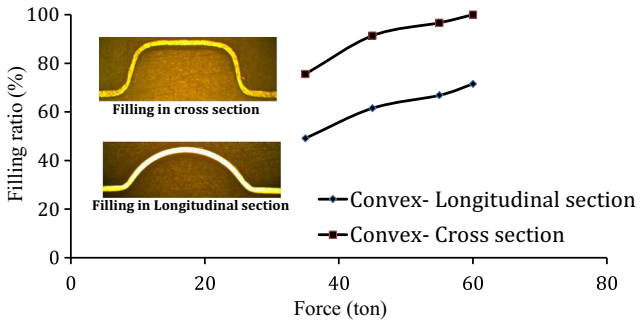

Fig. 17 Differences in depths of channel filling at longitudinal and cross-sectional directions in convex die

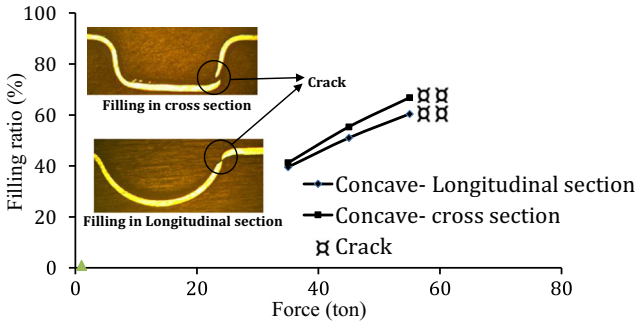

Fig. 18 Differences in depths of channel filling at longitudinal and cross-sectional directions in concave die

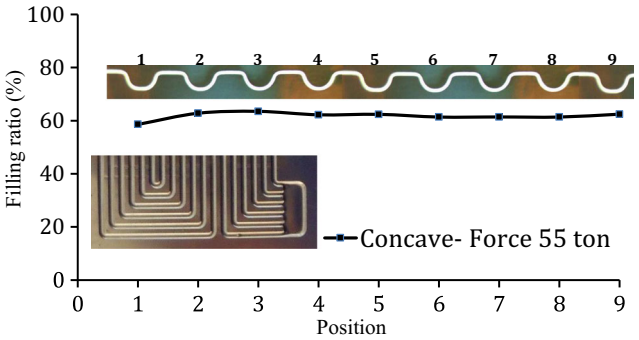

Fig. 20 Channel filling depths in different cutting situations longitudinally in concave die

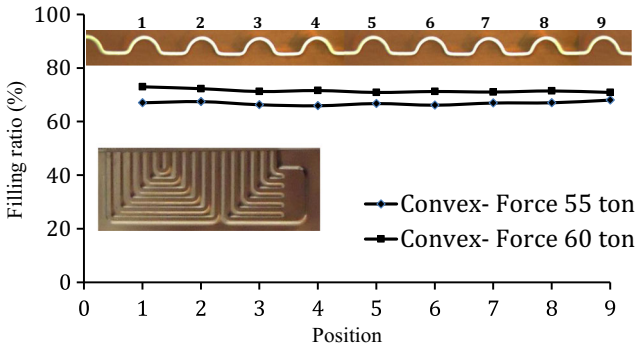

Fig. 19 Channel filling depths in different situations, cutting longitudinally in convex die

Table 7 Percentage of uniformity error in channel depths in concave die

Positions channel	55 tons
h_1	5.16
h_2	1.65
h_3	2.78
h_4	0.67
h_5	0.96
h_6	0.68
h_7	0.62
h_8	0.67
h_9	1.08

sheet into the channel. Overall, the maximum percentage of filling depth was 49 % in the concave die, while it was 60 % in the convex one. Increasing the force to 60 tons caused tearing in longitudinal channels of produced plates in the concave die.

Figure 16 shows filling depths of bipolar plates in both convex and concave dies, from 35 to 60 tons. The ratio of filling at this direction to longitudinal direction in both models increased. It could be due to channels having more space in diagonal directions than the longitudinal ones (Fig. 9). This would cause the rubber to flow into channel pores, and the sheet to be conducted into the channel more easily. As a result, more filling depth was possible in cross-sectional direction than the longitudinal one.

The percentage of filling in diagonal direction in the plate produced by the convex die was 77 %, whereas it was 50 % in the formed work piece produced by the concave die.

Figures 17 and 18 show the differences in the amounts of filling in channel depths both longitudinally and diagonally in both convex and concave dies, respectively. The maximum difference between channel depths in diagonal and

Table 6 Percentage of uniformity error in channel depths in convex die

Positions channel	55 tons	60 tons
h_1	0.28	2.07
h_2	0.92	1.09
h_3	0.81	0.38
h_4	1.38	0.1
h_5	0.16	0.87
h_6	1.05	0.38
h_7	0.14	0.66
h_8	0.28	0.09
h_9	1.78	0.87

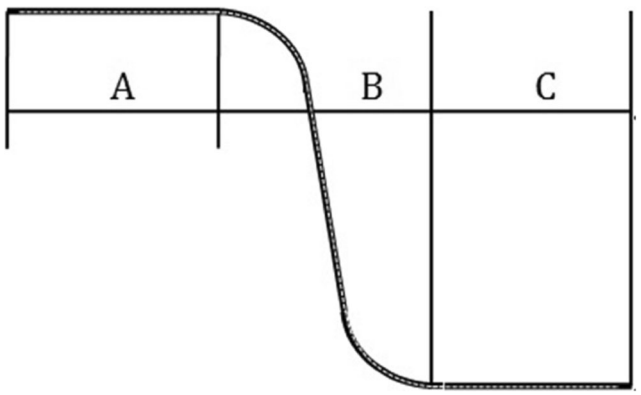

Fig. 21 Sheet thickness in three regions of channel

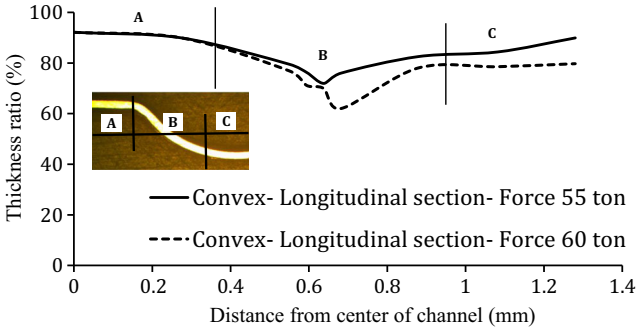

Fig. 22 Measuring sheet thickness in three regions of channel in convex die, longitudinally

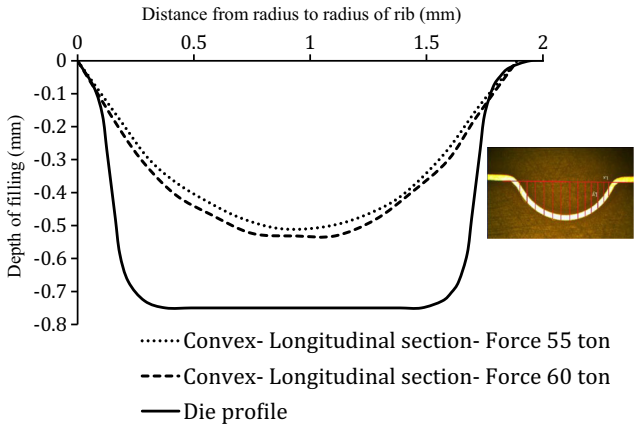

Fig. 23 Filling profile samples of convex die, longitudinally

longitudinal directions in the convex die was 28.5 %. However, in the concave die, the difference in the formed work piece without any defects was 8 %, which indicated filling uniformity in the concave pattern compared with the convex one.

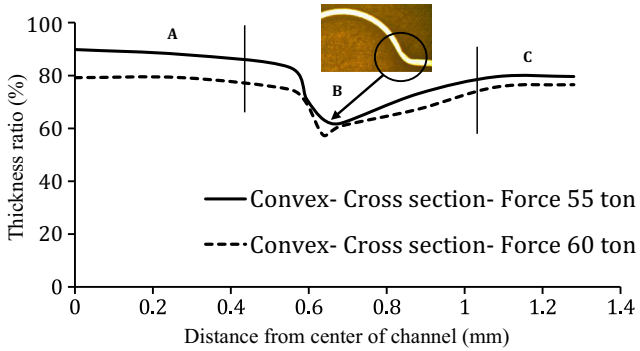

Fig. 24 Measuring sheet thickness in three regions of channel in convex die, diagonally

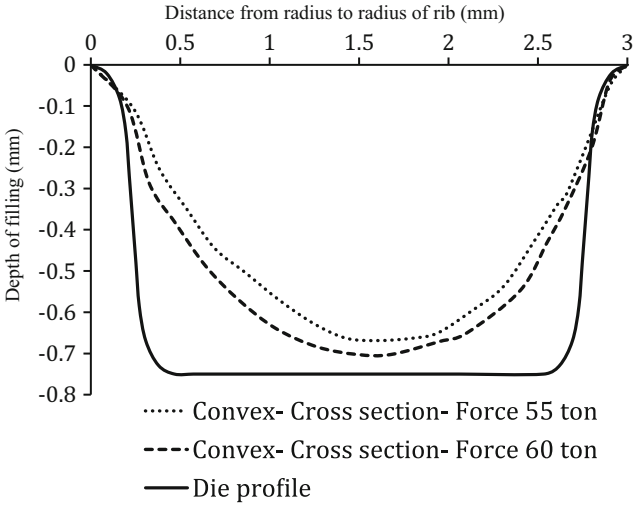

Fig. 25 Filling profile samples of convex die, cross-sectionally

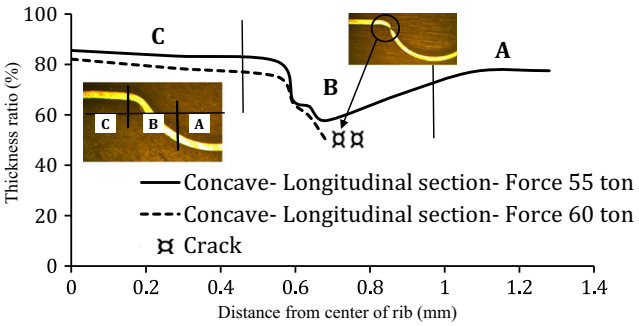

Fig. 26 Measuring sheet thickness in three regions of channel in concave die, longitudinally

6 Dimensional precision

One of the advantages of forming bipolar plates is having the same depth in channels. In other words, all channels should have the same filling depth or the same tolerance region in order to avoid problems in the function of plates in fuel cells.

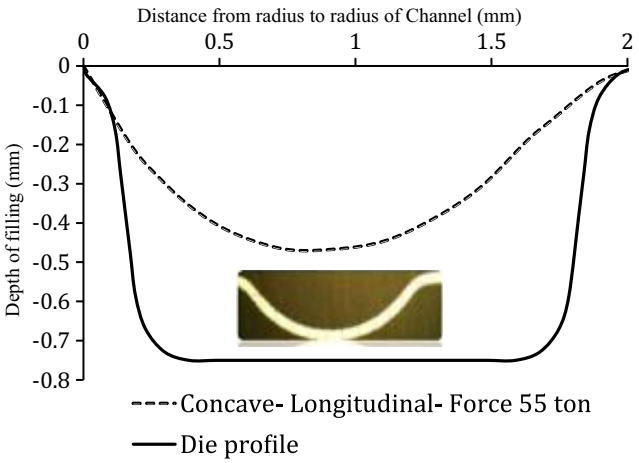

Fig. 27 Filling profile samples of concave die, longitudinally

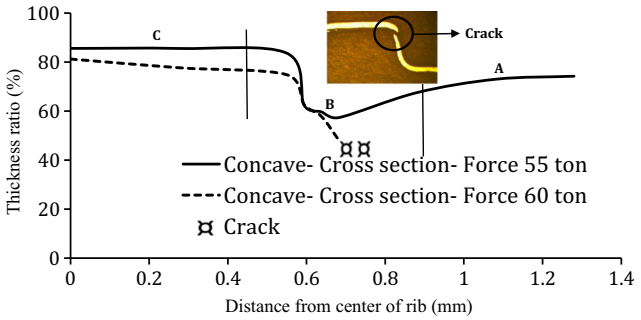

Fig. 28 Measuring sheet thickness in three regions of channel in concave die, cross-sectionally

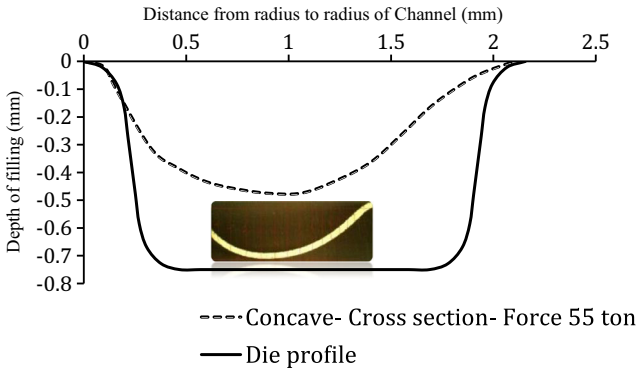

Fig. 29 Filling profile samples of concave die, cross-sectionally

Fluid pressure in the channels with the same depth would be uniform; however, in plates with unequal channel depths, it would cause inequality in system pressure. Otherwise, the performance and life of a fuel cell would decline.

Figure 19 provides information about channel depth uniformity in the convex die. To investigate the accuracy of bipolar plate channels, formed sheets were longitudinally cut (Fig. 19). The depths of channels were measured at nine separate positions, i.e. three channels to the left (h_1, h_2, h_3), three in the middle (h_4, h_5, h_6), and three to the right (h_7, h_8, h_9).

Equation (7) was used to study the errors resulting from channel depth uniformity. In this equation, (e) represents the percentage of error function. The average depth of measured channels from 1 to 9 was (h_m), and (h_k), showing the channel depth at each position. Table 6 presented the percentage of error in each channel from 55 to 60 tons with maximum filling amounts. As can be seen, error mean is less than 1 %, shown in Fig. 19 as well.

$$e = [(|h_m - h_k|)/h_m] \times 100 \quad (7)$$

Figure 20 presents data on uniformity of channel depths in the concave die. Table 7 shows the percentage of error in each channel at 55 tons, which was the highest force in this study. A comparison between Table 7 and Fig. 20 shows that channel depth in the concave die showed more dispersal compared with the convex one. As a result, the error mean obtained from the concave die was more than 1.5 %, whereas it was less than 1 % in the convex one. However, both die patterns contained required dimensional accuracy.

7 Thickness distribution and filling profile

In order to study tearing points in the samples, both convex and concave patterns, the thickness of the samples was measured in three different regions of the channel and then compared with their primary thickness (0.1 mm) (Fig. 20). The three regions, i.e., A, B, and C were half channel width (A), up and down corner radius (B), and half rib width (C), respectively.

Figure 21 illustrates sheet thickness distributions in three areas of the channel in the convex die longitudinally at 55 and 60 tons. As clear, increasing forces would cause more filling

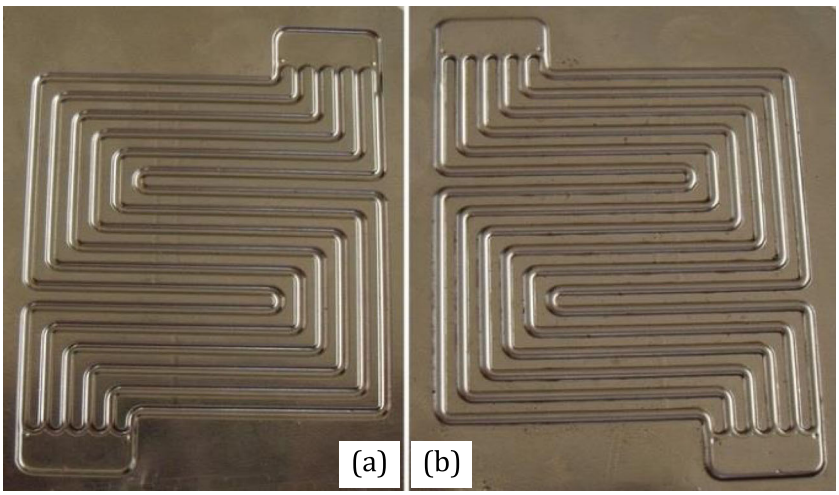

Fig. 30 Sample metal bipolar plate fabricated by rubber pad forming through concave die: **a** front view and **b** back view

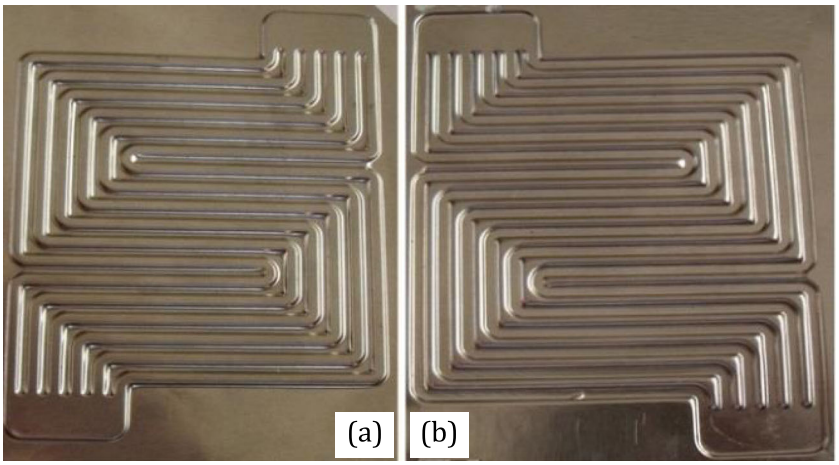

Fig. 31 Sample metal bipolar plate fabricated by rubber pad forming through convex die: **a** front view and **b** back view

in channel depths as well as making the sheet thinner. The thinnest part was in B region, at 0.074 mm, achieved at 60 tons. Thinning percentage was 26 % based on Eq. (1).

Longitudinal filling profiles of the convex sample at 55 and 60 tons are shown in Fig. 22. As can be seen, an increase in the force would cause the filling depth of the channel to rise. Before the sheet filled the groove completely, increasing the exerted force would tear the plate at top corner radius (in region B). This could cause sheet profile in the longitudinal direction to resemble a circular curve, not completely a die shape.

Diagonal thickness distribution of the work piece generated by the convex die is illustrated in Fig. 23, at 55 and 60 tons. Generally, the highest filling was obtained at 60. The thickness was measured in three different regions of the channel. The measured amounts are shown in Fig. 23, in which section B is the critical region based on the least thickness, and upper corner radius R, at 0.068 mm.

Figure 24 presents diagonal filling profile of the convex sample at 55 and 60 tons. As can be seen, when the forming force increases to more than 60 tons, more congestion will occur, but tearing will appear in the longitudinal direction of the channel.

Figure 25 shows longitudinal thickness distribution of the sample in the concave pattern at 55 and 60 tons. As clear, the work piece is measured at three separated areas of the channel; the data are added to this figure as well. The thinnest part was in B region, 0.069 mm, at 60 tons. Thinning percentage was 31 % based on Eq. (1). A force of 60 tons would lead to a tear in the wall and the floor of the channel. When force increased, the pressure applied by the rubber sheet rose as well. Since it was formed in the concave channel whose width was less than the width of the transmission channel congestion, the depth was less than the convex one. As the depth of the concave channel filling was less than the convex one, the sheet would approach tearing. The percentage of thinning near the tearing point was 34 %.

Figure 26 shows filling profile of the sample in the concave pattern; 55 tons was the maximum force the sheet would be able to withstand. The profile in this figure also illustrates the maximum depth of filling which the sheet could withstand, without any defect.

Figure 27 illustrates diagonal thickness distribution of the concave sample at 55 and 60 tons. As can be seen, the minimum thickness of 0.068 mm was reached according to Eq. (1). The thinning percentage of the diagonally manufactured plate by the concave pattern was 32 %, not noticeably different from the longitudinally produced one. As previously shown in Fig. 17, there was a small difference in the depths of filling between the longitudinal and diagonal methods, hence filling uniformity in the concave pattern. As a result, the thickness distributions of the two directions were very close to each other. The thickness near cracks or the thickest critical point was 0.067 mm, and the percentage of thinning was 33 %.

The process of channel profile filling in the concave pattern was similar to the longitudinal mode, showing the best final profile (Figs. 28 and 29).

Table 8 Final geometrically generated plates

Geometric parameters	Concave plate (%)	Convex plate (%)
Filling in longitudinal direction	49	60
Filling in diagonal direction	50	77
The maximum percentage of thinning in longitudinal direction	32	26
The maximum percentage of thinning in cross direction	32	31
Filling the difference between in the longitudinal and cross direction	8	28.5
Dimensional precision error	1.5	1

8 Produced plates

The main goal of this research was to produce metallic bipolar plates through rubber pad forming process with maximum filling, and minimum thinning, as well as the highest quality and the lowest cost. Although either concave or convex pattern can be used to produce bipolar plates, this study created both of the patterns to obtain uniformity and desired geometrical plates.

Figures 30 and 31 show the produced plates by both concave and convex dies with highest filling and lowest thinning, respectively. Table 8 presents the geometric measurements of the final plates.

9 Conclusions

The effectiveness of concave and convex patterns in forming metallic bipolar plates was investigated by rubber pad forming. Stainless steel316 sheets with the thickness of 0.1 mm were used. To form the plates, a PU with the hardness of shore A 85 and the thickness of 25 mm, as well as two dies of convex or concave patterns were used.

The effect of different forces on the formation of micro-channel filling depths was studied, in addition to the distribution of channel thickness in each of the patterns. From both patterns suitable forming parameters were obtained. The results indicated that in similar geometry and process, a convex die would create a deeper channel compared wiht a concave one. Moreover, the former would produce a thicker surface, hence more preferable to the latter.

Results also showed that by increasing forming force, the filling depth of micro-channels would rise. However, the thickness of the critical region would decrease due to an increase in aspect ratio. Finally, suitable conditions for bipolar plates in both convex and concave models were obtained.

Results:

1. At the same geometry and process, using a concave die would result in forming the surface of anode and cathode being completely flat, but the formation of the flow channel was not complete. Conversely, in the convex die flow channel perfectly formed, while the surface formation of cathode and anode was not complete.
2. In similar geometry and process, the convex die created a deeper channel compared with the concave one. Filling depth in the former was 60 %, while it was 49 % in the latter.
3. Since the concave die created a thicker surface, it could be preferable to the convex one.
4. The complexity index of forming at the ratio of 0.7 clearly showed that the convex pattern would be better than the concave one. Since a deeper pattern was created in the convex pattern, the distribution of bipolar plates could be acceptable.
5. Increasing forming forces would result in rising filling depths in both concave and convex patterns. Distribution of channel thickness showed that at 60 tons, most critical points would be achieved in the convex pattern along the longitudinal direction of 0.074 mm. However, tearing occurred at this force at the sides and the bottom of channels in the concave die. Minimum thickness of sheets in the convex die at 60 tons was 0.068 mm at diagonal direction, although the maximum filling depth happened at this direction as well.

References

1. Ministry of Iran. Renewable energy organization of Iran. Accessed 11 June 2015; http://www.suna.org.ir/
2. Ma L, Warthesen S, Shores DA (2000) Evaluation of materials for bipolar plates in PEMFCs. J New Mater Electrochem Syst 3:221–228
3. Wang H, Turner JA (2010) Reviewing metallic PEMFC bipolar plates. Fuel Cells 10:510–519
4. Mehta V, Cooper JS (2003) Review and analysis of PEM fuel cell design and manufacturing. J Power Sources 114:32–53
5. Kwon HJ, Jeon YP, Kang CG (2013) Effect of progressive forming process and processing variables on the formability of aluminium bipolar plate with microchannel. Int J Adv Manuf Technol 64:381–394
6. Osia MB, Bakhshi-Jooybari M, Hosseinipour SJ, Gorgi A (2015) A new process of forming metallic bipolar plates for PEM fuel cell with pin-type pattern. Int J Adv Manuf Technol 77:1281–1293
7. American Society for Metals (1988) Metals handbook. Forming and forging, 9th edition, vol. 14, 605–615.
8. Liu Y, Hua L (2010) Studies of the deformation styles of the rubber-pad forming process used for manufacturing metallic bipolar plates. J Power Sources 195:8177–8184
9. Jeong MG, Jin CK, Hwang GW, Kang CG (2014) Formability evaluation of stainless steel bipolar plate considering draft angle of die and process parameters by rubber forming. J Precis Eng Manuf 15:913–919
10. Son C-Y, Jeon Y-P, Kim Y-T, Kang C-G (2012) Evaluation of the formability of a bipolar plate manufactured from aluminum alloy Al 1050 using the rubber pad forming process. J Eng Manuf 226:909–918
11. Dundar F, Dur E, Mahabunphachai S, Koc M (2010) Corrosion resistance characteristics of stamped and hydroformed proton exchange membrane fuel cell metallic bipolar plates. J Power Sources 195(11):3546–3552
12. Mahabunphachai S, Cora ÖN, Koc M (2010) Effect of manufacturing processes on formability and surface topography of proton exchange membrane fuel cell metallic bipolar plates. J Power Sources 195(16):5269–5277
13. Aue-U-Lan Y, Ngaile G, Altan T (2004) Optimizing tube hydroforming using process simulation and exprimental verification. J Mater Process Technol 146:137–143